

and of Hulm¹⁴ (hatched curve), which was examined by Ulbrich *et al.*, is also shown in Fig. 2. These data fall below our theoretical prediction, though they exceeded the original prediction (see Fig. 2) of Ulbrich *et al.* by approximately a factor of 2. That these data fall below those of Gueths *et al.* as well as below our own prediction is not at all surprising; their data were taken on polycrystalline samples, for which an orientation effect might easily explain the discrepancy.

CONCLUSION

We have used the ideas contained in the theory of Ulbrich *et al.*, along with the expression derived by Kadanoff and Martin, together with some plausible interpretations of experimental data involving the conduction electrons. We have shown that the theory of the effect of superconductivity on the thermal con-

ductivity is in good agreement with existing experimental data. Because our estimation of the distribution of electronic velocities and energy gap is neither precise nor immune to criticism, we can not claim decisive victory over the K_e^s/K_e^n ratio. However, we can insist that the present theory does explain this ratio in tin within the uncertainty of our knowledge about the thermal current carriers.

ACKNOWLEDGMENTS

We gratefully thank Professor Paul Klemens, who suggested attributing conduction properties to certain limited regions of the Fermi surface, and who continued to lend his interest to this analysis. We also wish to thank Michael Mitchell for assistance with computer programming, and Ronald Linz for preparing the illustrations. The computational part of this work was carried out in the Computer Center at the University of Connecticut, which is supported in part by Grant GP-1819 of the National Science Foundation.

¹⁴ J. K. Hulm, Proc. Roy. Soc. (London) A204, 98 (1950).

Theory of Superconductor-Normal-Metal Interfaces

W. L. McMILLAN*

Bell Telephone Laboratories, Murray Hill, New Jersey and Cavendish Laboratory, Cambridge, England

(Received 18 December 1967)

The superconducting properties of the clean superconductor-normal-metal interface are calculated assuming a constant BCS potential $\Delta(x)$ in the superconductor and zero potential in the normal metal. We evaluate the local electronic density of states, which is measured in the tunneling experiments, and find the magnitude of the interference-effect oscillations. The BCS potential is recalculated and is believed to be nearly self-consistent. The pair amplitude $\langle \psi^+(x)\psi^+(x) \rangle$ and the potential oscillate $\propto \cos(x/\xi)$ in the normal metal. We suggest a Josephson tunneling experiment to measure the pair amplitude.

I. INTRODUCTION

WE present a solution of perhaps the simplest problem in space-dependent superconductivity: the superconductor-normal-metal (SN) interface.^{1,2} We consider the planar semi-infinite geometry of Fig. 1 with a superconductor to the left of $x=0$ and a normal metal to the right. We work at zero temperature, neglect impurity scattering, and assume that except for the interaction leading to superconductivity the two metals are identical free-electron gases.

The superconductivity theory^{3,4} is a self-consistent field theory in which the BCS potential $\Delta(\mathbf{x})$ is to be

determined self-consistently. We begin with a reasonable guess for this potential (constant in S and zero in N) and calculate the wave functions (or the Green's functions). The potential is then recalculated from these Green's functions from the self-consistency equation⁴

$$\Delta(\mathbf{x}) = \lambda^*(\mathbf{x})F(\mathbf{x}), \quad (1)$$

where λ^* is the effective pairing interaction and $F(\mathbf{x})$ is the pair amplitude

$$F(\mathbf{x}) = \langle \Psi^\dagger(\mathbf{x})\Psi^\dagger(\mathbf{x}) \rangle \quad (2)$$

in the usual notation.

The motivation for this work is a desire to calculate the magnitude of the interference effect oscillations found by Tomasch⁵ and by Rowell⁶ in the tunneling

* Supported in part by the Science Research Council, London.

¹ P. D. DeGennes and D. Saint-James, Phys. Letters 4, 151 (1963).

² D. S. Falk, Phys. Rev. 132, 1576 (1963).

³ J. Bardeen, L. N. Cooper, and J. R. Schrieffer, Phys. Rev. 106, 162 (1957); 108, 1175 (1957).

⁴ L. P. Gor'kov, Zh. Eksperim. i Teor. Fiz. 34, 735 (1958) 36, 1918 (1959) [English transl.: Soviet Phys.—JETP 7, 505 (1958); 9, 1364 (1959)].

⁵ W. J. Tomasch, Phys. Rev. Letters 15, 672 (1965); 16, 16 (1966).

⁶ J. M. Rowell and W. L. McMillan, Phys. Rev. Letters 16, 453 (1966).

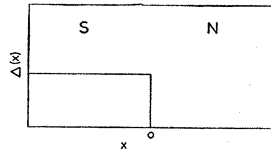


FIG. 1. Starting BCS potential for the semi-infinite planar SN interface.

density of states of SN sandwiches. These oscillations⁷ arise from the interference between incoming and scattered quasiparticle states where the scattering takes place at the interface. One finds a term in the local electronic density of states at energy E (which is what is measured in the tunneling experiment) proportional to $\cos[2(E^2 - \Delta^2)^{1/2}d/\hbar v_F]$ where Δ , d , and v_F are the energy gap, the thickness, and the Fermi velocity of the superconductor. The energy and thickness dependence of the oscillations have already been verified experimentally.^{5,8} Here we calculate the magnitude of the oscillations for the Tomasch geometry (tunneling into the S side of the SN sandwich) and suggest that the magnitude be measured experimentally. The calculation of the magnitude for the Rowell geometry (tunneling into the N side) was included in a previous paper.⁶

We have in addition found in the potential and pair amplitude an oscillatory term proportional to $(\xi/x)^{5/2} \cos(x/\xi)$, where ξ is the coherence length, which is the superconducting analog of the Friedel oscillations⁹ in the Hartree potential. We suggest an experiment, the measurement of the magnitude of the dc Josephson current¹⁰⁻¹² though a tunnel junction placed on the N side, which, in principle, directly measures the pair amplitude at the tunneling surface.

The plan of the paper is as follows. In Sec. II we review the theory of superconductivity and discuss the scattering states. In Sec. III the single-particle Green's functions are calculated and in Sec. IV the measurement of the electronic density of states by tunneling is discussed. In Sec. V we calculate the potential and the pair amplitude and in Sec. VI we discuss the measurement of the pair amplitude by Josephson tunneling.

II. THEORY OF NONUNIFORM SUPERCONDUCTIVITY

We begin with a discussion of the theory of superconductivity, emphasizing those aspects of the theory which will be useful for us. The superconducting state is a phase of a metal which is characterized by the existence

of bound Cooper pairs of electrons. The formal structure of the theory put forward by Bardeen, Cooper, and Schrieffer is rather simple, being a generalization of the Hartree self-consistent-field (SCF) method. In the Hartree method one takes account of the scattering of one electron from the average potential $V(\mathbf{x})$ created by the other electrons as illustrated pictorially in Fig. 2(a). One chooses a trial Hartree potential, calculates the electronic wave functions in that potential, and then recalculates the potential from the self-consistency equation. In the superconducting state an additional process must be taken into account; one must allow for the condensation of two electrons into a bound Cooper pair [Fig. 2(b)] with amplitude $\Delta(\mathbf{x})$. It turns out that one can twist this process around into a single-particle scattering process from a self-consistent potential $\Delta(\mathbf{x})$ [Fig. 2(c)]. It is evident from that picture that an electron comes in, is scattered from $\Delta(\mathbf{x})$, and goes out as a hole. Of course what has in fact occurred is that the incoming electron has found another electron inside the Fermi sea to pair with leaving a hole excitation. The theory of superconductivity is nothing more than a generalization of the Hartree SCF by including the self-consistent potential $\Delta(\mathbf{x})$ which scatters electrons into holes. The excited states of the metal, instead of being one-electron states, are now mixtures of an electron and a hole and are described by a two-component wave function

$$\Psi(\mathbf{x}) = \begin{pmatrix} u(\mathbf{x}) \\ v(\mathbf{x}) \end{pmatrix}, \quad (3)$$

where $u(\mathbf{x})$ is the electron amplitude and $v(\mathbf{x})$ is the hole amplitude. This quasiparticle wave function satisfies the following wave equation:

$$\begin{aligned} [-(\hbar^2/2m)\nabla^2 - \mu + V(\mathbf{x})]u(\mathbf{x}) + \Delta(\mathbf{x})v(\mathbf{x}) &= Eu(\mathbf{x}), \\ [(\hbar^2/2m)\nabla^2 + \mu - V(\mathbf{x})]v(\mathbf{x}) + \Delta(\mathbf{x})u(\mathbf{x}) &= Ev(\mathbf{x}), \end{aligned} \quad (4)$$

where E is the energy of the quasiparticle relative to the chemical potential μ . It is convenient to take advantage of the small parameter $\Delta/E_F \sim 10^{-4}$ and to introduce at an early stage an approximation used by Andreev.¹³ We choose $V(\mathbf{x})$ to be a constant and assume that $\Delta(\mathbf{x})$ is a

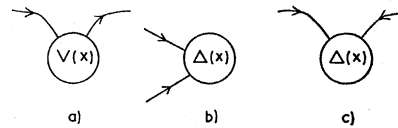


FIG. 2. (a) Electron scattering from the Hartree potential. (b) Two electrons condensing into a Cooper pair. (c) Electron scattering from the BCS potential into a hole.

⁷ W. L. McMillan and P. W. Anderson, Phys. Rev. Letters **16**, 85 (1966).

⁸ W. J. Tomasch and T. Wolfram, Phys. Rev. Letters **16**, 352 (1966).

⁹ J. Friedel, Phil. Mag. **43**, 153 (1952); Nuovo Cimento Suppl. **2**, 287 (1958).

¹⁰ B. D. Josephson, Phys. Letters **1**, 251 (1962); Advan. Phys. **14**, 419 (1965).

¹¹ P. W. Anderson and J. M. Rowell, Phys. Rev. Letters **10**, 230 (1963).

¹² P. W. Anderson, in *Progress in Low Temperature Physics*, edited by C. J. Gorter (Elsevier Publishing Co., Inc., Amsterdam, 1966), Vol. 5.

¹³ A. F. Andreev, Zh. Eksperim. i Teor. Fiz. **46**, 1823 (1964) [English transl.: Soviet Phys.—JETP **19**, 1228 (1964)].

function of x only. Then writing

$$\begin{aligned} u(\mathbf{x}) &= \bar{u}(\mathbf{x}) \exp(i\mathbf{k}_F \cdot \mathbf{x}), \\ v(\mathbf{x}) &= \bar{v}(x) \exp(i\mathbf{k}_F \cdot \mathbf{x}), \end{aligned} \quad (5)$$

where \bar{u} and \bar{v} are smooth on the atomic scale of length, we find

$$\begin{aligned} - (i\hbar^2 k_{Fz}/m) (d/dx)\bar{u}(x) + \Delta(x)\bar{v}(x) &= E\bar{u}(x), \\ (i\hbar^2 k_{Fz}/m) (d/dx)\bar{v}(x) + \Delta(x)\bar{u}(x) &= E\bar{v}(x), \end{aligned} \quad (6)$$

by dropping the d^2/dx^2 term which is of order Δ/E_F relative to the d/dx term. The matching conditions on \bar{u} and \bar{v} are simplified because one requires only that the wave functions be continuous. This approximation eliminates the scattering of quasiparticles with positive k_{Fz} into states with negative k_{Fz} , which is permitted by momentum conservation but can in fact be neglected.

Now suppose that we have thick planar slabs of a normal metal and a superconductor in good metallic contact along the plane $x=0$. As our first guess for the self-consistent BCS potential we might choose

$$\begin{aligned} \Delta(x) &= \Delta, & x < 0 \\ &= 0, & x > 0 \end{aligned} \quad (7)$$

where Δ is the bulk energy gap of the superconductor. Our next task is to set about solving for the wave functions of (6) with this potential. In the superconductor there are two solutions with energy E

$$\Psi_{\pm} = \begin{pmatrix} 1 \\ \Delta/(E \pm \Omega) \end{pmatrix} \exp(\pm i\Omega x/\hbar v_{Fz}), \quad x < 0 \quad (8)$$

$$\begin{aligned} \Omega &= (E^2 - \Delta^2)^{1/2}, & E > \Delta \\ &= i(\Delta^2 - E^2)^{1/2}, & E < \Delta \end{aligned} \quad (9)$$

corresponding to the two degenerate quasiparticle states in the excitation spectrum of Fig. 3(a). For $E > \Delta$ the states are propagating plane wave states and for $E < \Delta$ the states decay exponentially with x . In the normal metal [Fig. 3(b)] there are two solutions, the electron

$$\Psi_e = \begin{pmatrix} 1 \\ 0 \end{pmatrix} \exp(iEx/\hbar v_{Fz}), \quad (10)$$

and the hole

$$\Psi_h = \begin{pmatrix} 0 \\ 1 \end{pmatrix} \exp(-iEx/\hbar v_{Fz}). \quad (11)$$

In order to find the wave functions of the system we must match the solutions at $x=0$. Suppose we wish to find the transmission probability of a quasiparticle in the superconductor approaching the interface. In S the wave function is a linear combination of the incoming quasiparticle Ψ_+ and the outgoing quasiparticle Ψ_- and in N there is the outgoing electron Ψ_e .

$$\begin{aligned} \Psi &= \Psi_+ + a\Psi_-, & x < 0 \\ &= b\Psi_e, & x > 0. \end{aligned} \quad (12)$$

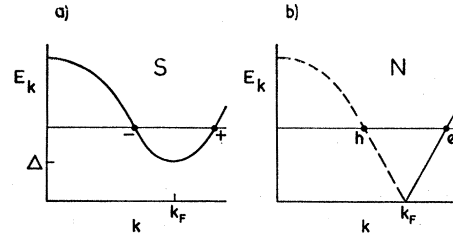


FIG. 3. (a) Single-particle excitation spectrum of a superconductor. (b) Single-particle excitation spectrum of a normal metal; (---) holes and (—) electrons.

Matching the amplitudes of the wave functions at $x=0$ we find

$$a = (\Omega - E)/(\Omega + E), \quad b = 2\Omega/(\Omega + E), \quad (13)$$

and the transmission probability

$$T = 4E\Omega/(\Omega + E)^2, \quad (14)$$

which goes to unity at high energy where the propagator modifications are small and goes to zero for $E = \Delta$. The wave function in the superconductor is

$$\begin{aligned} \bar{v}(x) &= \exp(i\Omega x/\hbar v_{Fz}) + (\Omega - E)/(\Omega + E) \\ &\quad \times \exp(-i\Omega x/\hbar v_{Fz}), \\ \bar{u}(x) &= [\Delta/(E + \Omega)] [\exp(i\Omega x/\hbar v_{Fz}) \\ &\quad - \exp(-i\Omega x/\hbar v_{Fz})]. \end{aligned} \quad (15)$$

The interference between the incoming and outgoing waves produces a term proportional to $\cos(2\Omega x/\hbar v_{Fz})$ in the amplitude of the wave function and leads to the Tomash-Rowell oscillations in the electronic density of states.

The vanishing of the transmission probability for $E = \Delta$ has an amusing consequence for certain finite geometries. Consider the BCS potential of Fig. 4(a) in which $\Delta(x) = \Delta$ for $-d < x < 0$ and vanishes otherwise. A quasiparticle in S with energy slightly greater than Δ will be nearly perfectly reflected at both interfaces and the eigenstates will be virtual bound states. According to (15) the wave function approximately vanishes at both interfaces and is

$$\bar{u}(x) = \bar{v}(x) = \sin(\Omega x/\hbar v_{Fz}), \quad (16)$$

with the eigenvalue condition

$$\Omega d/\hbar v_{Fz} = n\pi. \quad (17)$$

The spacing between the energy levels is

$$dE/dn = [(E^2 - \Delta^2)/E]^{1/2} (\hbar v_{Fz} \pi/d), \quad (18)$$

and the width of the levels is

$$\Gamma \approx (dE/dn) T, \quad (19)$$

so that the virtual bound states are well defined whenever $T \ll 1$, that is, for $(E - \Delta)/\Delta \ll 1$.

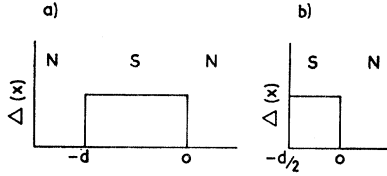


FIG. 4. (a) Finite geometry with virtual bound states in S. (b) Equivalent geometry with reflecting plane (tunneling surface) at $x = \frac{1}{2}d$.

How might these levels be observed? The geometry of Fig. 4(a) is equivalent to that of Fig. 4(b) with a perfectly reflecting plane at $x = -\frac{1}{2}d$. The virtual bound states would then appear in the local electronic density of states at the reflecting plane and could be observed in a tunneling experiment. Note that only the n -odd levels have a finite amplitude at $x = -\frac{1}{2}d$, so that the spacing between the levels observed in the tunneling experiment would be

$$dE/dn = [(E^2 - \Delta^2)/E]^{1/2} (\hbar v_{Fz} 2\pi/d), \quad (20)$$

which is identical to the period of the interference-effect oscillations. Of course the two effects are not distinct. The interference effect oscillations require only one reflection from the SN interface and produce a smooth oscillation in the density of states whereas the virtual bound states require many coherent reflections from both the SN interface and the tunneling surface and produce sharp structure in the density of states. In superposed films it seems likely that the electron mean free path is short enough to destroy the many coherent reflections necessary to produce the virtual bound states, and thus one will observe only the smooth oscillations.

III. CALCULATION OF SINGLE-PARTICLE PROPERTIES

In this section we calculate the single-particle properties, for example, the local electron density of states, of the SN geometry of Fig. 1. We could proceed as in Sec. II to compute the eigenfunctions and eigenvalues of (4) with appropriate boundary conditions and then perform the sum over states to find the density of states. It is, in fact, simpler to write the single-particle Green's functions which then provide the desired information. Another advantage of the Green's-function method is that one can use the "strong-coupling"¹⁴⁻¹⁶ form of the theory, which is known to be accurate for metals, instead of working with the BCS model.

We work with the Nambu¹⁴ spinor Green's functions,

¹⁴ Y. Nambu, Phys. Rev. **117**, 648 (1960).

¹⁵ G. M. Eliashberg, Zh. Eksperim. i Teor. Fiz. **38**, 966 (1960) [English transl.: Soviet Phys.—JETP **11**, 696 (1960)].

¹⁶ J. R. Schrieffer, *Theory of Superconductivity* (W. A. Benjamin, Inc., New York, 1964).

where the field operator is a two-component spinor

$$\Psi(\mathbf{x}) = \begin{pmatrix} \psi_1(\mathbf{x}) \\ \psi_1^\dagger(\mathbf{x}) \end{pmatrix}, \quad (21)$$

and the Green's function is a 2×2 matrix defined by

$$G(\mathbf{x}, t, \mathbf{x}', t') = -i \langle 0 | T \{ \Psi(\mathbf{x}, t) \Psi^\dagger(\mathbf{x}', t') \} | 0 \rangle, \quad (22)$$

where $|0\rangle$ is the ground state in the Heisenberg representation and T is the Wick time ordering operator. The 11 component of G is the ordinary electron Green's function and the 12 component is the Gorkov's "anomalous" Green's function. The problem is translationally invariant in the y and z directions and it is convenient to Fourier transform the Green's function in those coordinates and in the time variable

$$G(k_\perp, E, x, x') = \int \exp[-i\mathbf{k}_\perp(\mathbf{x}-\mathbf{x}') + iE(t-t')] \times G(\mathbf{x}, t, \mathbf{x}', t') dy dz dt. \quad (23)$$

G satisfies the following wave equation in x with a similar equation in x' :

$$[E\tau_0 - (-\hbar^2/2m)(d^2/dx^2) + \mu_x]\tau_3 - \Sigma(E, x)] \times G(k_\perp, E, x, x') = \delta(x-x')\tau_0, \quad (24)$$

where τ_0 is the 2×2 unit matrix and τ_1, τ_2 , and τ_3 are the Pauli matrices and $\mu_x = \mu - \hbar^2 k_\perp^2 / 2m$. According to the strong-coupling theory the matrix self-energy is of the form

$$\Sigma(E, x) = (Z(E, x) - 1)E\tau_0 + \phi(E, x)\tau_1, \quad (25)$$

where Z is the renormalization function and ϕ is the pairing self-energy. One writes

$$\Delta(E, x) = \phi(E, x)/Z(E, x) \quad (26)$$

and $\Delta(E, x)$ plays the role of the BCS potential. The self-consistency equations for Z and ϕ are given in Sec. V. As in Sec. II we take ϕ and Z constant and equal to their bulk values in S and $\phi=0, Z=1$ in N .

$$\begin{aligned} Z(E, x) &= Z(E), & x < 0 \\ &= 1, & x > 0 \\ \phi(E, x) &= \phi(E), & x < 0 \\ &= 0, & x > 0. \end{aligned} \quad (27)$$

The Green's function is made up of products of solutions (in x and x') of the wave equation with the appropriate incoming or outgoing boundary conditions. In S for fixed E and k_\perp there are four solutions, proportional to $\exp(\pm ik_{Fz}x \pm iZ\Omega x/\hbar v_{Fz})$, with $\Omega = [E^2 - \Delta^2(E)]^{1/2}$. As discussed in the Sec. II one can ignore the mixing of the $\exp(\pm ik_{Fz}x)$ components and simply match the amplitude of the waves at the interface. Consider first the $\exp(ik_{Fz}x)$ components. The solution with outgoing boundary conditions to the

right is [Eqs. (12) and (13)]

$$\Psi_{\text{out}}^{(+)}(x) = \exp(ik_{Fz}x) \left[\begin{pmatrix} 1 \\ \Delta/(E+\Omega) \end{pmatrix} \exp(iZ\Omega x/\hbar v_{Fz}) \right. \\ \left. + (\Omega-E)/(\Omega+E) \begin{pmatrix} 1 \\ \Delta/(E-\Omega) \end{pmatrix} \exp(-iZ\Omega x/\hbar v_{Fz}) \right], \quad x < 0 \quad (28)$$

and the solution with incoming boundary conditions to the left is

$$\Psi_{\text{in}}^{(+)}(x') = \exp(ik_{Fz}x') \begin{pmatrix} 1 \\ \Delta/(E+\Omega) \end{pmatrix} \exp(iZ\Omega x'/\hbar v_{Fz}), \quad x' < 0. \quad (29)$$

The Green's function for $x' < x < 0$ is proportional to the direct product of these solutions plus the appropriate term from the $\exp(-ik_{Fz}x)$ components,

$$G \propto \Psi_{\text{out}}^{(+)}(x)\Psi_{\text{in}}^{(+)\dagger}(x') + \Psi_{\text{out}}^{(-)}(x)\Psi_{\text{in}}^{(-)\dagger}(x'). \quad (30)$$

Putting these pieces together we find

$$G(k_{\perp}, E, x, x') = i/2\hbar v_{Fz}\Omega \\ \times \left\{ \exp[ik_{Fz}(x-x')] \left[\exp[iZ\Omega(x-x')/\hbar v_{Fz}] \right. \right. \\ \times \begin{pmatrix} (E+\Omega) & \Delta \\ \Delta & (E-\Omega) \end{pmatrix} - \exp[iZ\Omega(-x-x')/\hbar v_{Fz}] \\ \times \begin{pmatrix} (E-\Omega) & \Delta(E-\Omega)/(E+\Omega) \\ \Delta & (E-\Omega) \end{pmatrix} \left. \right] + \exp[-ik_{Fz}(x-x')] \right. \\ \times \left[\exp[iZ\Omega(x-x')/\hbar v_{Fz}] \begin{pmatrix} (E-\Omega) & \Delta \\ \Delta & (E+\Omega) \end{pmatrix} \right. \\ \left. - \exp[iZ\Omega(-x-x')/\hbar v_{Fz}] \right. \\ \left. \times \begin{pmatrix} (E-\Omega) & \Delta \\ \Delta(E-\Omega)/(E+\Omega) & (E-\Omega) \end{pmatrix} \right] \left. \right\}, \quad x' < x < 0. \quad (31)$$

G satisfies the homogeneous wave equation in x and x' for $x \neq x'$ since it is made up of products of solutions. The normalization is fixed by requiring that the change in slope at $x=x'$ be equal to $2m/\hbar^2$ so that G satisfies (24). One finds G for $x < x' < 0$ from (31) by interchanging x and x' and transposing the matrices. It is

easily verified that G is properly normalized. A similar calculation yields G in N.

$$G(k_{\perp}, E, x, x') = i/\hbar v_{Fz} \\ \times \left\{ \exp[ik_{Fz}(x-x')] \left[\exp[iZE(x-x')/\hbar v_{Fz}] \begin{pmatrix} 0 & 0 \\ 0 & 1 \end{pmatrix} \right. \right. \\ \left. + \exp[iZE(x+x')/\hbar v_{Fz}] \begin{pmatrix} 0 & (E-\Omega)/\Delta \\ 0 & 0 \end{pmatrix} \right] \\ \left. + \exp[-ik_{Fz}(x-x')] \left[\exp[iZE(x-x')/\hbar v_{Fz}] \begin{pmatrix} 1 & 0 \\ 0 & 0 \end{pmatrix} \right. \right. \\ \left. + \exp[iZE(x+x')/\hbar v_{Fz}] \begin{pmatrix} 0 & 0 \\ (E-\Omega)/\Delta & 0 \end{pmatrix} \right] \left. \right\}, \quad 0 < x' < x. \quad (32)$$

According to the usual considerations the local electronic density of states is proportional to the imaginary part of the local ($x=x'$) Green's function (this is the ordinary Green's function, the 11 component of G).

$$N(k_{\perp}, E, x) = (\text{Im}/\pi) G_{11}(k_{\perp}, E, x, x). \quad (33)$$

From (31) and (32) we find

$$N_S(k_{\perp}, E, x) = (\pi\hbar v_{Fz})^{-1} \text{Re}\{E/\Omega - [(E-\Omega)/\Omega] \\ \times \exp(-2iZ\Omega x/\hbar v_{Fz})\}, \quad x < 0 \quad (34)$$

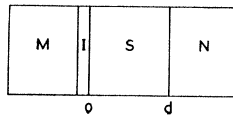
$$N_N(k_{\perp}, E, x) = (\pi\hbar v_{Fz})^{-1}, \quad x > 0. \quad (35)$$

There are two contributions to the Green's function in S. The first contribution is from waves propagating directly from x' to x [the first and third term of (31)] which is just the Green's function for the uniform superconductor. The second contribution is from waves originating at x' which scatter from the SN interface and then propagate to x . Similarly there are two contributions to the local electronic density of states (34), the bulk contribution (E/Ω) and the scattering contribution $[(E-\Omega) \exp(2iZ\Omega/\hbar v_{Fz})/\Omega]$. The oscillatory scattering term, which is of primary interest here, arises directly from the interference between the electron parts of the incident quasiparticle state Ψ_+ and the scattered quasiparticle state Ψ_- . In the normal metal an incident hole state Ψ_h is scattered into an electron state Ψ_e which has no overlap with Ψ_h and there is no interference effect, no scattering contribution in (35).

IV. TUNNELING EXPERIMENT

In this section we discuss the tunneling experiment and show that one measures the local electronic density of states at the tunneling surface weighted by the angular distribution of the tunneling electrons. We then

FIG. 5. Tomasch geometry with a tunnel junction placed on the S side of an SN sandwich.



calculate this "tunneling density of states" for the SN sandwich for both random and specular tunneling.

The geometry that we have in mind is the Tomasch geometry (Fig. 5) where one has a normal metal M, an insulator I, a superconductor S of thickness d in good metallic contact with a normal metal N. One measures the current I through the insulator or its derivatives versus voltage V . The electrons penetrate the insulating barrier by the quantum-mechanical tunneling process. We make use of the tunneling Hamiltonian method¹⁷ in which this barrier penetration is accomplished by an effective Hamiltonian that removes an electron from the left-hand metal near the tunneling surface and injects it into the right-hand metal near the tunneling surface. By treating this Hamiltonian in lowest-order time-dependent perturbation theory one finds that the current is proportional to the density of occupied electron states on the left (near the surface) times the matrix elements of the Hamiltonian squared times the density of available electron states on the right (near the surface). If the left-hand metal is in the normal state, the density of occupied states is constant for energies below the Fermi energy and zero above. For this case the first derivative of I versus V is directly proportional to the density of available states of the SN sandwich at the tunneling surface and weighted by the angular distribution of the tunneling electrons. We define the tunneling density of states

$$N_T(V) = (dI/dV)_S / (dI/dV)_N \quad (36)$$

to be the first derivative dI/dV versus V for the SN sandwich in the superconducting state normalized to dI/dV for the SN sandwich in the normal state. This tunneling density of states is then equal to the weighted average of the electronic density of states at the tunneling surface

$$N_T(E) = \int_0^{\pi/2} N_S(k_F \sin\theta, E, -d) D(\theta) \sin\theta d\theta, \quad (37)$$

where $D(\theta)$ is the normalized probability distribution of the tunneling electrons (for the normal state of the SN sandwich), θ is the angle between the electron momentum and the normal to the surface and we omit the factor $(\pi\hbar v_{Fz})^{-1}$ from N_S as found in (34). For the case of specular tunneling the electron distribution is Gaussian about $\theta=0$, reflecting the fact that the barrier-penetration probability is largest for electrons traveling normal to the surface.

$$D_{\text{spec}}(\theta) = \beta \exp(-\beta\theta^2/2), \quad \beta \sim 40. \quad (38)$$

For the case of tunneling with random scattering we take

$$D_{\text{rand}}(\theta) = 1. \quad (39)$$

By substituting (34) and (38) or (39) into (37) we

find for the tunneling density of states

$$N_T(E) = \text{Re} \{ (E/\Omega) - [(E-\Omega)/\Omega] \mathcal{G}(2Z\Omega d/\hbar v_F) \}, \quad (40)$$

where the interference factor for specular tunneling is

$$\begin{aligned} \mathcal{G}_{\text{spec}}(y) &\cong \beta e^\beta \int_1^\infty \exp[(iy-\beta)x] \frac{dx}{x^2} \\ &\cong e^{iy} / [1 - (iy/\beta)], \end{aligned} \quad (41)$$

and for random tunneling

$$\mathcal{G}_{\text{rand}}(y) = \int_1^\infty e^{iyx} \frac{dx}{x^2}. \quad (42)$$

The interference factors are unity for $y=0$ and fall off as $(\exp iy)/iy$ for large y .

The tunneling density of states is plotted in Fig. 6 for specular tunneling with $d=4(\hbar v_F/2Z\Delta)$. For $E < \Delta$ one is observing the tails of the normal metal states that decay exponentially into the superconductor with a characteristic length $\hbar v_F/Z(\Delta^2 - E^2)^{1/2}$ that becomes shorter as the energy is lowered; the density of states is unity for $E = \Delta$ and oscillates about the bulk density of states with period $\delta E = \pi\hbar v_F(1 - \Delta^2/E^2)^{1/2}/Zd$ as predicted earlier and verified experimentally. The amplitude of the oscillations is of order unity for E near Δ and falls off as E^{-3} at high energy.

There are two strong-coupling effects: (a) According to the theory, Δ and Z are energy-dependent leading to a weak energy dependence of $\delta E/(1 - \Delta^2/E^2)^{1/2}$ which has probably been observed.⁷ Of course the Fermi velocity that enters the theory is the quasiparticle Fermi velocity v_F/Z which contains the renormalization due to the electron-phonon interaction. This renormalization is henceforth suppressed. (b) For electron energies comparable to typical phonon energies, the electron states are severely broadened by phonon emission. The imaginary part of Z becomes important and the magnitude of the oscillations is reduced by the factor $\exp[-2Z\Omega d/\hbar v_F]$ which is just $\exp[-d/l_{\text{ph}}(E)]$, where $l_{\text{ph}}(E)$ is the electron mean free path due to phonon emission.

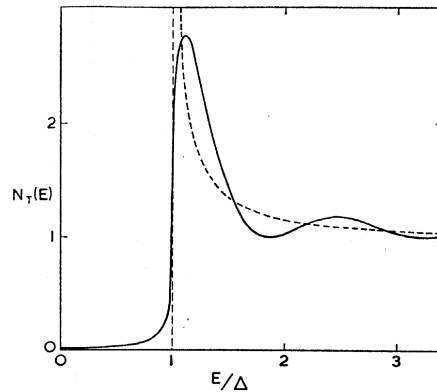


FIG. 6. Calculated tunneling density of states for the Tomasch geometry (Fig. 5) with specular tunneling and $d=4\xi$ (—) and for the bulk superconductor (---).

¹⁷ M. H. Cohen, L. M. Falicov, and J. C. Phillips, Phys. Rev. Letters **8**, 316 (1962).

V. SELF-CONSISTENT POTENTIAL AND PAIR AMPLITUDE

Having discussed the calculation of the wave functions for a particular BCS potential, we now turn to the recalculation of the potential as the first step toward self-consistency. We will find that the new potential is not very different from the assumed potential (7) and is therefore very nearly self-consistent. In addition we show that on the N side the potential and the order parameter oscillate with distance from the SN interface as

$$F(x) \sim \Delta \left[-\frac{1}{8}(\xi/x)^2 - (\xi/x)^{5/2} \cos(x/\xi - \frac{3}{4}\pi) \right], \quad (43)$$

where ξ is the coherence length $\hbar v_F/2\Delta$, which is $\frac{1}{2}\pi$ longer than the usual coherence length ξ_0 . This oscillation of the order parameter is the analog for the superconductor of the Friedel oscillations about a discontinuity in the Hartree potential for the normal metal. An experiment is proposed for the observation of this order-parameter oscillation.

We begin with a discussion of the self-energy equations (the self-consistency equations) of the theory of superconductivity. The interaction between electrons takes place via the exchange of virtual phonons and the screened Coulomb term. Both interactions are short ranged in space¹⁸ with range of order the interatomic distance or the screening, length, much shorter than the coherence length. It is therefore a good approximation to consider a δ -function interaction in real space. However the phonon contribution is highly retarded in time leading to a strong energy dependence of the self-energy equations. The self-energy, within second-order self-consistent perturbation theory (Fig. 7), is

$$\begin{aligned} \phi(E, x) &= \int_0^\infty dE' \frac{\text{Im}}{\pi} G_{12}(E', x, x) \\ &\quad \times [K^+(E, E', x) - \mu^*], \\ [Z(E, x) - 1]E &= \int_0^\infty dE' \frac{\text{Im}}{\pi} G_{11}(E', x, x) K^-(E, E', x), \end{aligned} \quad (44)$$

where the kernel for the phonon-induced interaction is

$$\begin{aligned} K^\pm(E, E', x) &= \int_0^\infty d\omega \alpha^2 G(\omega, x) \\ &\quad \times [(E' + E + \omega - i\delta)^{-1} \pm (E' - E + \omega - i\delta)^{-1}], \end{aligned} \quad (45)$$

and $\alpha^2 G$ is an averaged electron-phonon matrix element

FIG. 7. Phonon and Coulomb contributions to the matrix self-energy for the superconducting state.

squared times the phonon density of states. The Coulomb term is represented by a pseudopotential μ^* with an energy cutoff at a typical phonon energy. We take $\alpha^2 G$ and μ^* equal to the bulk value in S and zero in N. The self-consistency equation for $\Delta = \phi/Z$ is then

$$\begin{aligned} \Delta(E, x) &= [Z(E, x)]^{-1} \int_0^\infty dE' \frac{\text{Im}}{\pi} G_{12}(E', x, x) \\ &\quad \times [K^+(E, E', x) - \mu^*]. \end{aligned} \quad (46)$$

The dominant contribution to the integral is from low energy and we write approximately

$$\Delta(x) \cong \lambda^*(x) \int_0^{E_{c0}} dE' \frac{\text{Im}}{\pi} G_{12}(E', x, x), \quad (47)$$

where

$$\begin{aligned} \lambda^*(x) &= [K^+(0, 0, x) - \mu^*]/Z(0, x) \\ &= (\lambda - \mu^*)/(1 + \lambda). \end{aligned} \quad (48)$$

Here λ is the dimensionless electron-phonon coupling constant and λ^* is just the $N(0)V$ of the BCS model. The integral of (47) is cut off at E_{c0} in order to cure the logarithmic divergence. Equations (47) and (24) are just Gor'kov's equations for the BCS model with an energy cutoff.

In order to recalculate the BCS potential $\Delta(x)$ we take the expressions for G_{12} from (31) and (32) and perform the energy and angular integrals. Introducing the pairing amplitude or order parameter $F(x)$,

$$\Delta(x) = \lambda^*(x)F(x), \quad (49)$$

where

$$F(x) = \int_0^{E_{c0}} dE \frac{\text{Im}}{\pi} G_{12}(E', x, x), \quad (50)$$

we find in S

$$\begin{aligned} F_S(x) &= \text{Re} \int_0^{E_{c0}} dE \\ &\quad \times \int d \cos\theta \left[\frac{\Delta}{\Omega} - \frac{\Delta E \exp(-2i\Omega x/\hbar v_F \cos\theta)}{\Omega(E+\Omega)} \right] \\ &= F_{\text{bulk}} - \int_1^\infty \frac{dy}{y^2} \int_{i\Delta}^\infty \frac{E-\Omega}{\Delta} \exp(iy|x|\Omega/\xi\Delta) d\Omega \\ &= F_{\text{bulk}} - \frac{x}{\xi} \int_{x/\xi}^\infty \frac{dy}{y^2} I_S(y), \end{aligned} \quad (51)$$

with

$$I_S(y) = [(1/y) + (1/y^2)]e^{-y} + \frac{1}{2}\pi[H_1^{(1)}(iy)/y]. \quad (52)$$

The integral definitions of the Hankel function above and of the Bessel function below are from Janke and Emde,¹⁹ and numerical values are to be found therein.

¹⁸ P. Morel and P. W. Anderson, Phys. Rev. **125**, 1273 (1962).

¹⁹ E. Jahnke and F. Emde, *Tales of Functions* (Dover Publications, Inc., New York, 1945), p. 150.

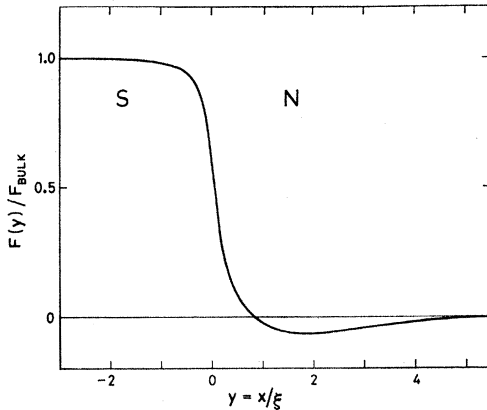


FIG. 8. Pair amplitude for the SN interface at zero temperature. The oscillatory term which appears at larger distances is not visible on the scale of this graph.

In N we find similarly

$$F_N(x) = \text{Re} \int_0^{E_{c0}} dE \times \int_0^1 d \cos \theta \left[\frac{E - \Omega}{\Delta} \exp(2iEx/\hbar v_F \cos \theta) \right] = \frac{x}{\xi} \int_{x/\xi}^{\infty} \frac{dy}{y^2} I_N(y), \quad (53)$$

where

$$I_N(y)^{-1} = -(y^2)^{-1} - \frac{1}{2}\pi [N_1(y)/y]. \quad (54)$$

For reasonable values of x/ξ the integrals of the oscillatory terms in (51) and (53) converge and the cutoff is unnecessary. However, for very small y both I_S and I_N diverge logarithmically. The proper limit for $x=0$ is

$$F(0) = \frac{1}{2}\Delta [\ln(2E_{c0}/\Delta) + \frac{1}{2}], \quad (55)$$

which is somewhat greater than one-half the bulk value

$$F_{\text{bulk}} = \Delta \ln(2E_{c0}/\Delta). \quad (56)$$

In (51) and (53) we cut off I_S and I_N for $y \approx 2E_{c0}/\Delta$.

The final integration in (51) and (53) is readily performed by hand and we find the curve for $F(x)$, normalized by F_{bulk} , shown in Fig. 8 [for $\ln(2E_{c0}/\Delta) = 2.3$]. The pairing amplitude approaches the bulk value very quickly (exponentially) for $x < 0$, is roughly half the bulk value at $x=0$, then drops rapidly for $x > 0$ finally approaching

$$F(x) \sim \Delta \left\{ -\frac{1}{8}(\xi/x)^2 - (\xi/x)^{5/2} \cos[(x/\xi) - \frac{3}{4}\pi] \right\} \quad (57)$$

for large x . The oscillatory term arises from the singularity in the electronic reflection amplitude for $E = \Delta$. For $E < \Delta$ an electron in N approaching the interface is totally reflected whereas for $E > \Delta$ there is some probability that the electron will be transmitted into S. At this energy the incoming and outgoing states have a phase difference $\delta\phi = 2\Delta x/\hbar v_F$, and an oscillatory term $\alpha \exp i\delta\phi$ is introduced in the pairing amplitude and in

the potential (for finite λ^*). In S this singularity occurs for infinite wavelength and there are no oscillatory terms. The physical origin of these oscillations in the potential is therefore somewhat different from the Friedel case where the oscillations arise from the momentum-space cutoff in the occupation number. The Friedel oscillations $\propto \cos(2k_F x)$ have a wavelength comparable to the characteristic length k_F^{-1} of the normal metal; they persist unmodified in the superconducting state. The oscillations in the BCS potential have a wavelength comparable to the characteristic length of the superconducting state, the coherence length.

The recalculated BCS potential (Fig. 9) is just λ^* times $F(x)$ in S and zero in N. This potential is not very different from the assumed potential, indicating that the potential is now nearly self-consistent. A quantitative measure of that difference is

$$(\Delta\xi)^{-1} \int_{-\infty}^0 [\Delta - \Delta(x)] dx = 0.25/\ln(2E_{c0}/\Delta), \quad (58)$$

which is of order 0.05 to 0.1. We expect further higher corrections to $\Delta(x)$ to be of order 10% of the correction that we have just calculated.

At finite temperatures Eqs. (51) and (53) are modified by including the usual factor of $\tanh(E/2T)$ under the energy integral. At low temperature the x^{-2} term in (57) is cut off for x of the order of the thermal wavelength $\hbar v_F/2T$, whereas the oscillatory term is reduced only by the factor $\tanh(\Delta/2T)$.

Near T_c the Ginzburg-Landau (GL) theory is valid in the superconductor for distances greater than ξ_0 from the interface. The BCS potential varies over the GL scale of length

$$\xi(T) = 0.74\xi_0 [T_c/(T_c - T)]^{1/2} \gg \xi_0$$

and (7) is not a good starting function for a self-consistent calculation. The calculational procedure used for $T=0$, which depends on (7) being reasonably close to the self-consistent solution, breaks down near T_c . However, following DeGennes and co-workers,²⁰ we can

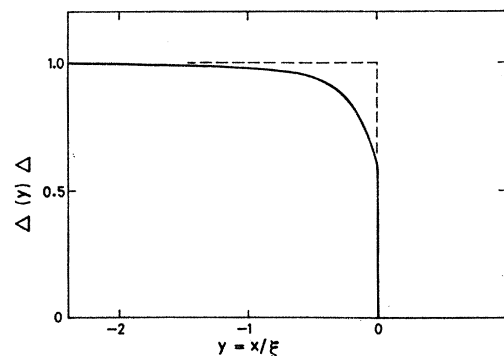


FIG. 9. Recalculated BCS potential for the SN interface (—) together with the starting potential (---).

²⁰ P. G. DeGennes, *Superconductivity of Metals and Alloys* (W. A. Benjamin, Inc., New York, 1966).

make use of the GL theory deep in the superconductor and use the linearized integral equation for Δ near the interface to find the self-consistent $\Delta(x)$ and $F(x)$. According to the GL theory $\Delta(x)$ is of the form²⁰

$$\Delta(x) = \Delta_{\text{bulk}}(T) \tanh[(-x + b\xi_c)/\sqrt{2}\xi(T)] \quad (59)$$

deep in the superconductor, where b is of order one. Near the interface $\Delta(x)$ is small, so that we can neglect higher order terms in Δ and solve the linear integral equation

$$\Delta(x) = \int_{-\infty}^0 K(x-x') \Delta(x') dx', \quad x < 0 \quad (60)$$

where the kernel for the clean superconductor is

$$K(x) = \frac{\lambda^* 2\pi T_c}{\hbar v_F} \sum_n \int_1^{\infty} \frac{dz}{z} \exp[-(2n+1)|x|z/\xi_c], \quad (61)$$

and the range of the kernel is

$$\xi_c = \hbar v_F / 2\pi T_c = 0.88\xi_0. \quad (62)$$

We will solve the integral equation by iteration taking

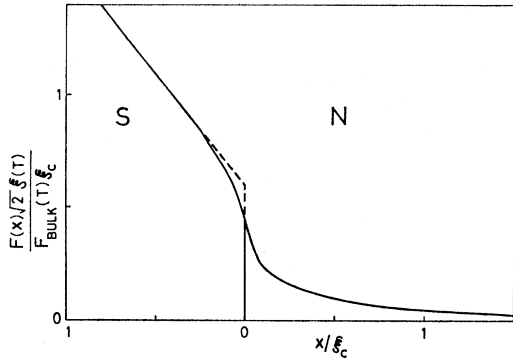


FIG. 10. Solid line is the pair amplitude near T_c normalized to unit slope in S. The dashed line is $\Delta^{(0)}(x)$ and the solid line in S is $\Delta^{(1)}(x)$; $\Delta(x)$ vanishes in N.

the starting solution from (59)

$$\begin{aligned} \Delta^{(0)}(x) &= \Delta_{\text{bulk}}(T) (-x + b\xi_c)/\sqrt{2}\xi(T), & x < 0 \\ &= 0, & x > 0. \end{aligned} \quad (63)$$

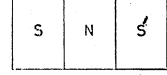
The first iterate of the integral equation is

$$\begin{aligned} \Delta^{(1)}(x) &= \int_{-\infty}^0 K(x-x') \Delta^{(0)}(x') dx' \\ &= \Delta^{(0)}(x) + \frac{\lambda^* \Delta_{\text{bulk}}(T) \xi_c}{\sqrt{2}\xi(T)} \left[f_1\left(\frac{-x}{\xi_c}\right) - b f_2\left(\frac{-x}{\xi_c}\right) \right], \end{aligned} \quad (64)$$

where

$$f_1(y) = \sum_n \frac{1}{(2n+1)^2} \int_1^{\infty} \frac{dz}{z^2} \exp[-(2n+1)yz] \quad (65)$$

FIG. 11. Possible experimental configuration for studying the pair amplitude in N.



and

$$f_2(y) = \sum_n \frac{1}{(2n+1)} \int_1^{\infty} \frac{dz}{z^2} \exp[-(2n+1)yz]. \quad (66)$$

The integrals are evaluated in terms of exponentials, and the exponential integral function and the sums are easily performed by hand. We treat b as a disposable parameter which is adjusted to make $\Delta^{(1)}(x)$ as close as possible to $\Delta^{(0)}(x)$. The functions $f_1(y)$ and $f_2(y)$ are very similar in shape for $y > -0.3$ and we find by choosing $b=0.6$ that $\Delta^{(1)}(x)$ and $\Delta^{(0)}(x)$ agree within $\frac{1}{2}\%$ for $x < -0.3\xi_0$. Thus it appears that we have found a nearly self-consistent solution for $\Delta(x)$. The pair amplitude is proportional to $\Delta(x)$ in the superconductor and satisfies (60) in the normal metal as well. We find

$$\begin{aligned} F(x) &= \frac{F_{\text{bulk}}(T)}{\sqrt{2}\xi(T)} \left\{ -x + b\xi_c + \lambda^* \xi_c \left[f_1\left(\frac{-x}{\xi_c}\right) - b f_2\left(\frac{-x}{\xi_c}\right) \right] \right\}, & x < 0 \\ &= \frac{F_{\text{bulk}}(T)}{\sqrt{2}\xi(T)} \lambda^* \xi_c \left[f_1\left(\frac{x}{\xi_c}\right) + b f_2\left(\frac{x}{\xi_c}\right) \right], & x > 0. \end{aligned} \quad (67)$$

Deep in the normal metal the asymptotic form for $F(x)$ is

$$F(x) \sim [F_{\text{bulk}}(T)/\sqrt{2}\xi(T)] \lambda^* \xi_c^2 (1+b) \exp(-x/\xi_c)/x, \quad x \gg \xi_c. \quad (68)$$

$\Delta(x)$ and $F(x)$ are plotted in Fig. 10 for $\lambda^*=1/4.6$.

VI. MEASUREMENT OF PAIR AMPLITUDE

Since the supercurrent is carried by the pairs, one might expect to learn something about the pair amplitude by measuring the maximum supercurrent for a given geometry. Two experimental configurations come to mind. The first is that of the SNS' sandwich (Fig. 11), where one measures the current carried through the normal slab. In order to calculate that current one could compute the total energy of the sandwich as a function of the phase difference ϕ between the Δ of S and S' and then use the Josephson-Anderson relation

$$I = dN_1/dt = (1/\hbar) (\partial E/\partial \phi) \quad (69)$$

to find the supercurrent. The other configuration is that

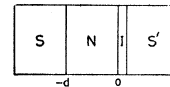


FIG. 12. Josephson junction placed on the N side of an SN sandwich to measure the pair amplitude in N at the tunneling surface.

of a Josephson tunnel junction placed on the N side of an SN sandwich, the SNIS' geometry (Fig. 12). We show here that under certain conditions the maximum supercurrent through the insulator is directly proportional to the pair amplitude at the tunneling surface. In principle, the measurement of the maximum Josephson current versus the thickness of the normal metal allows one to plot $F(x)$.

We calculate the maximum supercurrent using the tunneling Hamiltonian following Josephson¹⁰ and Anderson.¹²

$$H_T = \sum_{kq} T_{kq} (C_{k\uparrow} + C_{q\uparrow} + C_{-q\downarrow} + C_{-k\downarrow}) + \text{h.c.} \quad (70)$$

The total energy to second order,

$$\Delta E_2 = - \sum_n \frac{\langle 0 | H_T | n \rangle \langle n | H_T | 0 \rangle}{E_n}, \quad (71)$$

contains terms dependent on the phase difference between SN and S'.

$$\begin{aligned} \Delta E_2(\phi) = - \langle T^2 \rangle \sum_{mm'} \frac{\langle 0 | C_{k^+} | m \rangle \langle m | C_{-k^+} | 0 \rangle}{E_m + E_{m'}} \\ \times \langle 0 | C_q | m' \rangle \langle m' | C_{-q} | 0 \rangle + \text{c.c.}, \quad (72) \end{aligned}$$

where $|m\rangle$ and $|m'\rangle$ are exact excited states in SN and S', respectively, and we have replaced T_{kq}^2 by an averaged quantity. Now the quantity

$$\sum_k \sum_m \langle 0 | C_{k^+} | m \rangle \langle m | C_{-k^+} | 0 \rangle \delta(E - E_m) \quad (73)$$

is just the imaginary part of the anomalous Green's function evaluated at the tunneling surface. Physically, the tunneling process injects one electron at the tunneling surface and at some later time injects a second electron to form a bound pair. We find

$$\begin{aligned} \Delta E_2 = -2 \cos\phi \langle T^2 \rangle \int_0^\infty dE dE' \frac{\text{Im } G_{12}(E, x, x)}{E + E'} \\ \times \text{Im } G_{21}'(E', x, x), \quad (74) \end{aligned}$$

with x at the tunneling surface. Assuming that S' is a uniform superconductor with energy gap Δ' we have

$$\begin{aligned} \Delta E_2 = -2 \cos\phi \langle T^2 \rangle \int_0^\infty dE dE' \frac{\text{Im } G_{12}(E, x, x)}{E + E'} \\ \times \frac{\Delta'}{(E'^2 - \Delta'^2)^{1/2}}. \quad (75) \end{aligned}$$

Finally the main contribution to the E integral is from energies less than $\hbar v_F/d$, so that for $\hbar v_F/d \ll \Delta'$ we can neglect E relative to E' , in the denominator and find

$$\Delta E_2 = -\pi \cos\phi \langle T^2 \rangle F(x=0). \quad (76)$$

Using (69) the maximum dc supercurrent is

$$I_{\text{max}} = (\pi/\hbar) \langle T^2 \rangle F(x) = F(x=0)/4R, \quad (77)$$

where R is the junction resistance in the normal state. For the case of a reasonably thick normal-metal film and a reasonably large energy gap in S' the measurement of the maximum Josephson current and junction resistance determines the pair amplitude at the tunneling surface. Of course the presence of the tunneling surface modifies the pair amplitude from the results of Sec. V on the semi-infinite geometry. The SN sandwich with a normal metal of thickness d and specular scattering is equivalent to the SNS sandwich with a normal metal of thickness $2d$. For $d \gg \xi$ one can superpose the contributions to F from the left and right superconductors and we find that F at the tunneling surface for the SN case is just twice $F(d)$ for the semi-infinite case.

Since the maximum Josephson current between uniform superconductors is often less than one expects theoretically, perhaps one should attempt a relative measurement rather than an absolute one as suggested by (77). One could measure the current through a Pb-Al-I-Pb junction relative to an Al-I-Pb junction made at the same time to find the pair amplitude at the surface of the Pb-Al sandwich relative to Al.

The pair amplitude is negative at zero temperature and for $d > \xi$, and becomes positive at higher temperatures where the characteristic length becomes longer because of the temperature dependence of Δ and the thermal length becomes important. One would expect an anomaly in the Josephson current at the temperature where $F(d)$ passes through zero.

VII. CONCLUSION

We have presented a very nearly complete solution of the clean SN problem with semi-infinite geometry. We have computed the electronic density of states as a function of energy and distance from the interface and have found the magnitude of the interference-effect oscillations for the Tomasch geometry. Quantitative experiments for this geometry would be most interesting. A quantitative comparison of experiment and theory of the oscillations for the Rowell geometry is contained in Ref. 6. We have also recomputed the BCS potential and found that the potential is nearly self-consistent. The pair amplitude is found to oscillate in the normal metal and a Josephson tunneling experiment is suggested for its measurement.

The calculation was sufficiently simple so that it can probably be extended in several directions. One might want to include the effects of (1) impurity scattering, (2) reflection properties of the interface and (3) finite geometry. The properties of the clean SNS sandwich could be calculated by the above methods.

ACKNOWLEDGMENTS

The author would like to thank P. W. Anderson and J. M. Rowell for stimulating discussions.